AE AURIGAE: FIRST DETECTION OF NON-THERMAL X-RAY EMISSION FROM A BOW SHOCK PRODUCED BY A RUNAWAY STAR

J. LÓPEZ-SANTIAGO[1], M. MICELI[2,3], M. V. DEL VALLE[4], G. E. ROMERO[4,5], R. BONITO[2,3],
J. F. ALBACETE-COLOMBO[6], V. PEREIRA[1], E. DE CASTRO[1], AND F. DAMIANI[3]

[1] Dpto. de Astrofísica y CC. de la Atmósfera, Universidad Complutense de Madrid, E-28040 Madrid, Spain
[2] Dipartimento di Fisica, Università di Palermo, Piazza del Parlamento 1, I-90134 Palermo, Italy
[3] INAF-Osservatorio Astronomico di Palermo, Piazza del Parlamento 1, I-90134 Palermo, Italy
[4] Instituto Argentino de Radioastronomía (IAR), CCT La Plata (CONICET), C.C.5, 1894 Villa Elisa, Buenos Aires, Argentina
[5] Facultad de Ciencias Astronómicas y Geofísicas, Universidad Nacional de La Plata, Paseo del Bosque s/n, 1900 La Plata, Argentina
[6] Centro Universitario Regional Zona Atlántica (CURZA), Universidad Nacional del COMAHUE, Monseñor Esandi y Ayacucho,
8500 Viedma, Rio Negro, Argentina

ABSTRACT

Runaway stars produce shocks when passing through interstellar medium at supersonic velocities. Bow shocks have been detected in the mid-infrared for several high-mass runaway stars and in radio waves for one star. Theoretical models predict the production of high-energy photons by non-thermal radiative processes in a number sufficiently large to be detected in X-rays. To date, no stellar bow shock has been detected at such energies. We present the first detection of X-ray emission from a bow shock produced by a runaway star. The star is AE Aur, which was likely expelled from its birthplace due to the encounter of two massive binary systems and now is passing through the dense nebula IC 405. The X-ray emission from the bow shock is detected at 30″ northeast of the star, coinciding with an enhancement in the density of the nebula. From the analysis of the observed X-ray spectrum of the source and our theoretical emission model, we confirm that the X-ray emission is produced mainly by inverse Compton upscattering of infrared photons from dust in the shock front.

Key words: ISM: clouds – radiation mechanisms: non-thermal – stars: individual (AE Aur) – stars: kinematics and dynamics – stars: massive – X-rays: general

Online-only material: color figures

1. INTRODUCTION

Runaway stars move through space with an extremely high velocity relative to the surrounding interstellar medium (ISM; Blaauw 1961). A proposed scenario for the ejection of stars at high velocities from their birthplace is close interaction between two binary systems (e.g., Hoogerwerf et al. 2000). This process may produce ejection velocities close to the escape velocity at the surface of the most massive star in the system: up to 100–1000 km s^{-1} (Leonard 1991; Gvaramadze & Bomans 2008). The encounter of the proper motions of two or more stars favors the dynamical ejection scenario (Hoogerwerf et al. 2000). A typical example of a system of runaway stars escaping from a close interaction of two high-mass binaries is the group formed by AE Aur, μ Col, and ι Ori (e.g., Gualandris et al. 2004).

The passage of a runaway star excites the ISM forming a shock front (e.g., Mohamed et al. 2012) which acquires the characteristic shape of a bow. Several bow shocks were identified in the past with the *Infrared Astronomical Satellite* (*IRAS*; van Buren & McCray 1988; van Buren et al. 1995; Noriega-Crespo et al. 1997) and, more recently, with the *Spitzer Space Telescope* (Kobulnicky et al. 2010) and other infrared missions (e.g., Comerón & Pasquali 2007).

Recently, Benaglia et al. (2010) detected non-thermal radio emission in the massive runaway star BD+43° 3654. This emission was associated with the cooling of energetic electrons through synchrotron radiation and the authors hypothesized that some bow shocks may also produce high-energy emission that might be detectable. This problem was treated theoretically in del Valle & Romero (2012), who predicted detectable X-ray and gamma-ray emission associated with particle accel-

eration at the bow shock. No observational constraints to this phenomenon were found to date. Very recently, Terada et al. (2012) reported the non-detection of X-ray emission from the bow shock produced by BD+43° 3654 in a long-time exposure X-ray observation with *Suzaku*. In this Letter, we report the first detection of hard-energy emission from a bow shock.

2. THE RUNAWAY STAR AE Aur (HIP 24575)

AE Aur was ejected from its birthplace in the Orion Nebula cluster around three million years ago, very probably by the encounter of two massive binary systems. As a result, the stars AE Aur and μ Col (both with spectral type O9.5) were expelled at high velocities, while the system ι Ori remained as a bounded binary system with high eccentricity (Hoogerwerf et al. 2000).

AE Aur has recently encountered IC 405, a dense molecular nebula with hydrogen density $n_{\rm H} \sim 3\ \rm cm^{-3}$ (Peri et al. 2012). As a result of this encounter, a bow shock was produced. The bow shock was detected in the mid-infrared band by van Buren & McCray (1988) with *IRAS* and later by France et al. (2007) using *Spitzer*. Some important parameters of the star for our study are the terminal velocity of the wind ($v_{\infty} \approx 1500\ \rm km\ s^{-1}$; Hubrig et al. 2011), the mass-loss rate ($\dot{M} \sim 10^{-7}\ M_{\odot}\ \rm yr^{-1}$; Fullerton et al. 2006), and the velocity of the star ($v_{*} \approx 150\ \rm km\ s^{-1}$; Peri et al. 2012). In Table 1, we list a set of physical parameters of AE Aur, including some assumptions on the characteristics of relativistic particles adopted for our model.

3. X-RAY OBSERVATION AND DATA ANALYSIS

For our work, we analyzed the archival *XMM-Newton* EPIC observation of AE Aur (ID 0206360101, PI: F. Damiani),

Table 1
Parameters for the Non-thermal Radiative Model for AE Aur

Parameter		Value
R_0	Standoff radius	1.7×10^4 AU
$\dot{M}_w$	Wind mass-loss rate	$10^{-7}\ M_\odot$ yr^{-1}
a	Hadron-to-lepton energy ratio	1
q_{rel}	Content of relativistic particles	0.007
α	Particle injection index	2.6
V_w	Wind velocity	1.5×10^8 cm s^{-1}
L	Available power	4×10^{33} erg s^{-1}
B	Magnetic field	1.1×10^{-4} G
$V_\star$	Star velocity	150 km s^{-1}

performed on 2004 September 10 in Full Frame Mode with the medium filter. The data were processed with the Science Analysis System (SAS V12.0). Light curves, images, and spectra were created by selecting events with PATTERN $\leqslant$ 12 for the MOS cameras, PATTERN $\leqslant$ 4 for the pn camera, and FLAG = 0 for both. To reduce the contamination by soft proton flares, the original event files were screened by using the sigma-clipping algorithm (ESPFILT tasks). The screened MOS1/MOS2/pn exposure times are 52/54/38 ks, respectively. Spectral analysis was performed in the 0.3–7 keV energy band using XPEC V12.7 (the ancillary response files were generated with the SAS *ARFGEN* task). MOS and pn spectra were rebinned to achieve a signal-to-noise ratio per bin $>5\sigma$. All the reported errors are at the 90% confidence level.

Figure 1 shows the *WISE* 12.1 μm image (in red; see also Peri et al. 2012) of the bow shock of AE Aur together with the corresponding EPIC pn count image in the 1–8 keV band (top panel, in green) and the pn median photon energy map, i.e., an image where each pixel holds the median energy of the detected pn photons in the 0.3–8 keV band (bottom panel, in green; for details on the procedure adopted to produce the map, see Miceli et al. 2008). A bright X-ray source, $\sim$30′′ northwest of the star, is visible in the top panel of Figure 1 (BS region) and appears embedded in the infrared bow shock. We verified that BS has no point-like counterparts in the optical and infrared bands. The median photon energy map clearly shows that the X-ray emission from the BS source is significantly harder than that of AE Aur.[7] Namely, the average value of median photon energy is $\sim$850 eV in region BS and $\sim$750 eV in region AE Aur. Moreover, this map reveals a bow-shaped structure (not directly visible in the count image) characterized by hard X-ray emission and somehow reminiscent of the infrared bow shock.

We first analyzed the stellar spectrum by extracting the pn and MOS spectra from region "AE Aur" of Figure 1. We subtracted from the source spectrum a background spectrum extracted from a nearby region (out of the field of view of Figure 1). The fittings were performed simultaneously on both MOS spectra and on the pn spectrum by adopting an absorbed APEC model (optically thin coronal plasma in collisional ionization equilibrium; Smith et al. 2001) based on the 2.0 release of the AtomDB database. The interstellar absorption was described by the PHABS model in XSPEC. The stellar spectrum can be fitted (reduced $\chi^2 = 1.32$, with 315 dof) by an isothermal plasma with temperature $kT = 0.225^{+0.007}_{-0.004}$ keV, emission measure EM $= 2.8^{+0.5}_{-0.4} \times 10^{55}$ cm^{-3} (assuming a distance $D = 550$ pc,
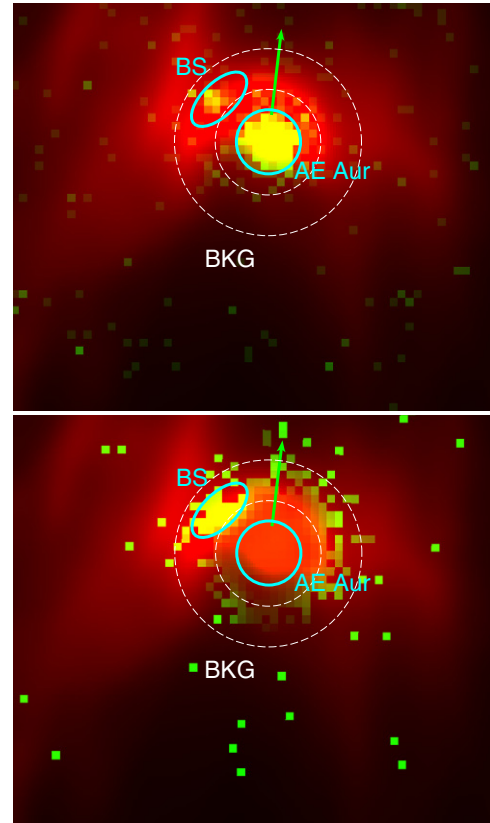
Figure 1. Top panel: *WISE* 12.1 μm image (red) and EPIC pn count image of AE Aur in the 1–8 keV band (green). The bin size of the X-ray image is 4′′. The regions selected for the spectral analysis and the proper motion vector are superimposed. BKG is the annular region from which the background spectrum was subtracted (see the text). North is up and east is to the left. Bottom panel: same as the top panel with pn median photon energy map in the 0.3–8 keV in green. In the median photon energy map, each pixel holds the median energy of the detected pn photons band. Only pixels with more than four counts were taken into account, and the image is smoothed with $\sigma = 8''$, according to the formulae in Miceli et al. (2008).

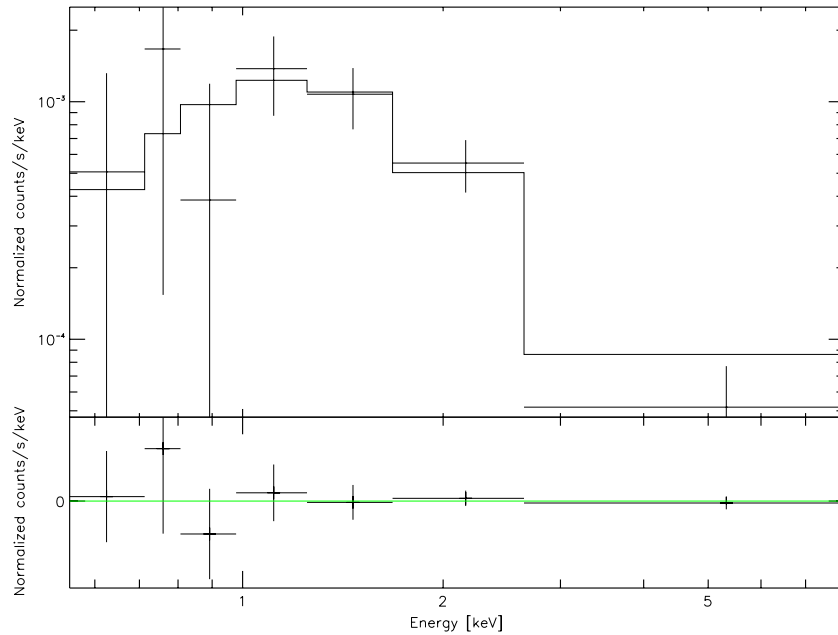(A color version of this figure is available in the online journal.)

in agreement with Peri et al. 2012), and oxygen abundance[8] O/O$_\odot = 0.26 \pm 0.02$. The best-fit value of the column density is $n_H = 4.2 \pm 0.2 \times 10^{21}$ cm^{-2} and the unabsorbed X-ray luminosity in the 0.3–10 keV band is $L_X = 1.9 \times 10^{32}$ erg s^{-1}.

We then analyzed the X-ray spectrum of the BS source (the extraction region is shown in Figure 1). The contamination from AE Aur photons scattered by the telescope point spread function in the BS region was removed by extracting the background spectrum from the region BKG of Figure 1. This region consists of an annulus centered at the star and with inner and outer radii that were chosen to contain pixels at the same distance from the star than the bow shock.[9] Figure 2 shows the pn spectrum of region BS. Only 180 pn counts (943 photon arcmin^{-2}) were detected in this region, while the spectra from the MOS cameras do not provide useful constraints and thus are not presented here. The BS spectrum can be well fitted by an absorbed power-law model with photon index $\Gamma = 2.6^{+0.6}_{-0.5}$ and normalization $N = 6 \pm 2 \times 10^{-6}$ photons keV^{-1} cm^{-2} s^{-1} at 1 keV. Since the absorbing column is consistent with that found for AE Aur, we

----

[7] We verified that the MOS cameras provide consistent results. Here we present pn images because of the better statistics.

[8] We verified that the plasma metallicity is $\sim$0.35 and we fixed the abundances of all other elements to this value.

[9] Pixels inside the BS region were extracted from the background extraction region (BKG).

Figure 2. Background-subtracted EPIC pn spectrum of region BS of Figure 1 with the theoretical model described in Section 4 and the corresponding residuals (observed–model).

(A color version of this figure is available in the online journal.)

fixed it to $n_H = 4.2 \pm 0.2 \times 10^{21}$ cm^{-2} in the fittings, to obtain tighter constraints on the other model parameters. We used Cash instead of χ^2 statistics for the fitting, which is recommended when the number of counts in a channel is small. We used the task *GOODNESS* with 1000 Monte Carlo simulations to determine the goodness of our fit. The value obtained for our fit is 2.3% of realizations with less best-fit statistic than that obtained with the fitted model (i.e., 97.7% confidence interval).

The BS spectrum can also be well fitted by a very hot thermal component with $kT = 2.4^{+2}_{-0.8}$ keV and EM $= 4 \pm 1 \times 10^{52}$ cm^{-3} (assuming that BS is at 550 pc). Such extremely high temperature cannot be associated with the stellar wind, as shown below. If we assume that the hot plasma fills the whole region, we derive from the EM a lower limit for the particle density, $n \sim 3$ cm^{-3}, which is much higher than that expected for a stellar wind.[10] Temperatures higher than 1.6 keV can be indicative of a cataclysmic variable star or of a very energetic coronal flare, though we verified that the BS light curve is consistent with a constant source. Given the low count rate of the source, statistical fluctuations are quite large and deeper exposures are necessary to obtain a proper study of the light curve. In conclusion, present data do not allow us to discriminate between a thermal and a non-thermal scenario for the BS X-ray emission and deeper observations are necessary. Nevertheless, the lack of infrared and optical counterparts and the extremely high temperature derived from the thermal model make the association of BS with a foreground/background stellar object less likely. On the contrary, the spatial correlation between BS and the infrared bow shock, the bow-shaped morphology of the hard X-ray emission around AE Aur, and the spectral properties of BS (see the next section) concur in suggesting that BS is indeed the result of non-thermal emission originating at the bow shock of the runaway star AE Aur.

---

[10] If the plasma does not fill the entire region we get even higher density values.

4. NON-THERMAL RADIATIVE MODEL

In order to explain the observed X-ray emission from the bow shock of AE Aur, we have applied the non-thermal radiative model of ζ Oph, developed by del Valle & Romero (2012) with the parameters given in Table 1 (see also Section 2). By adopting the stellar parameters of an O9.5V star and an ISM medium $N_H = 3$ cm^{-3} (Peri et al. 2012), we obtain that the runaway star produces a bow shock in the ISM with a stagnation point located at approximately 17.1×10^3 AU. This estimation agrees very well with the value measured from the X-ray observation ($\sim 17 \times 10^3$ AU). The reverse shock in the stellar wind is adiabatic and provides an efficient site for particle acceleration through a Fermi type I acceleration process. Since the gas is compressible, we assume that it is in sub-equipartition, getting an estimate of $\sim 10^{-4}$ G for the magnetic field in this medium (see del Valle & Romero 2012 for details).

The available power in the stellar wind is $\sim 4 \times 10^{33}$ erg s^{-1}. Assuming that only a small fraction of $\sim 1\%$ is transformed in relativistic particles (we assume equal power in leptons and hadrons), we have been able to reproduce the observed X-ray spectrum with a power-law electron injection of index -2.6, through inverse Compton upscattering of IR photons coming from dust that is heated by the forward shock and the thermal radiation. This model produces a good fit to the observed spectrum of the bow shock (see Figure 2), with reduced $\chi^2 = 0.43$ with 5 dof (see Section 2). Models with higher ratio of proton to electron power are possible. Since the cooling time of the protons is much longer, they are removed from the radiation zone without having time to make a significant contribution to the spectral energy distribution (SED). So, in order to keep the goodness of the fit, a larger total power is required for proton-dominated models. In a case similar to that of the Galactic cosmic rays, where the mentioned ratio is 100 instead of 1, we should consider that about 0.3 of the available power goes to relativistic particles. This requires very efficient acceleration. The case with $a = 1$ is energetically more conservative, but we
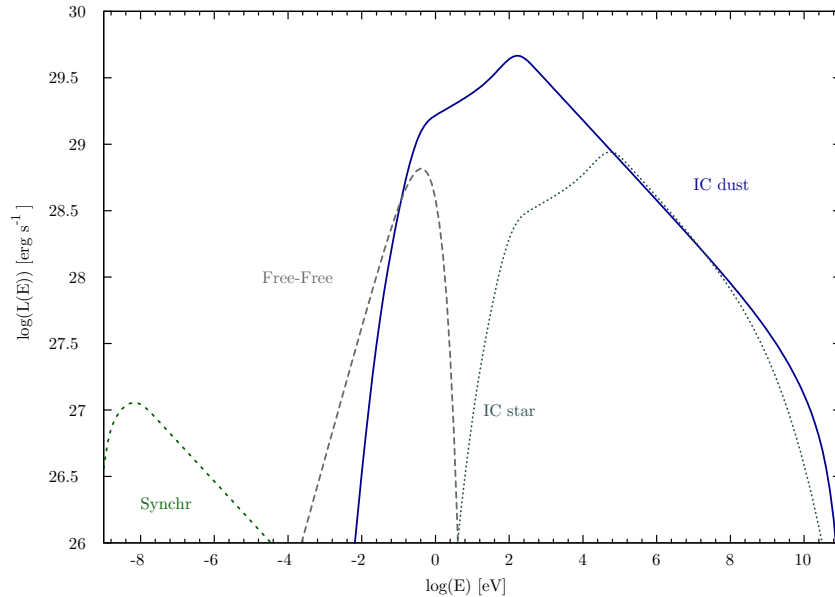
Figure 3. Spectral energy distribution of non-thermal radiative processes for the AE Aur bow shock. The model was computed following the work by del Valle & Romero (2012). The continuous line represents the inverse Compton process produced by the dust (see Section 4 for details).
(A color version of this figure is available in the online journal.)

cannot rule out models with a up to 100. In all cases, the shape of the SED is basically the same and determined by the electron population.

In Figure 3, we present the broadband SED implied by our model. Inverse Compton losses dominate, producing a steepening of the non-thermal spectrum that results in the soft power-law X-ray emission observed. The dominance of the radiative losses requires a low level of convection of the relativistic particles that can result from the development of Kelvin–Helmholtz instabilities in the bow shock (see conditions for these instabilities in bow shocks in Araudo et al. 2010).

The SED predicted for the runaway star has little and steep synchrotron radio emission and a peak of around $\sim 10^{29.5}$ erg s^{-1} at soft X-rays. Contrary to the case of ζ Oph, located closer and with different physical parameters, the expected emission at gamma rays is negligible. Hence, the best test for the proposed model is the radio detection through deep interferometric observations at long centimetric wavelengths.

5. CONCLUSION

We detected a hard X-ray source spatially correlated with the infrared bow shock of the runaway star AE Aur. The source is consistent with being a point-like steady source with non-thermal emission, though deeper observations are necessary to ascertain its morphology, its variability (if any), and its photon index. Nevertheless, the analysis of the X-ray source at $\sim 30''$ to the northeast of the runaway star AE Aur showed that it is very likely the X-ray counterpart of the bow shock produced by the passage of the star through the dense molecular nebula IC 405 and was detected in the infrared with *IRAS*, *Spitzer,* and *WISE*. We developed a radiative non-thermal model specifically tuned to describe the AE Aur bow shock properties and obtained a very good agreement between model and observations. According to our model, the X-ray emission would be produced by the inverse Compton process of accelerated particles in the nebula dust. High-energy emission from bow shocks produced by runaway stars has been predicted by theoretical models. This is the first

time that X-ray emission is detected in one of such bow shocks. Future X-ray and radio observations of this source will permit us to further constrain its properties.

REFERENCES

Araudo, A. T., Bosch-Ramon, V., & Romero, G. E. 2010, A&A, 522, A97
Benaglia, P., Romero, G. E., Martí, J., Peri, C. S., & Araudo, A. T. 2010, A&A, 517, L10
Blaauw, A. 1961, BAN, 15, 265
Comerón, F., & Pasquali, A. 2007, A&A, 467, L23
Del Valle, M. V., & Romero, G. E. 2012, A&A, 543, A56
France, K., McCandliss, S. R., & Lupu, R. E. 2007, ApJ, 655, 920
Fullerton, A. W., Massa, D. L., & Prinja, R. K. 2006, ApJ, 637, 1025
Gualandris, A., Portegies Zwart, S., & Eggleton, P. P. 2004, MNRAS, 350, 615
Gvaramadze, V. V., & Bomans, D. J. 2008, A&A, 485, L29
Hoogerwerf, R., de Bruijne, J. H. J., & de Zeeuw, P. T. 2000, ApJ, 544, L133
Hubrig, S., Oskinova, L. M., & Schöller, M. 2011, Astron. Nachr., 332, 147
Kobulnicky, H. A., Gilbert, I. J., & Kiminki, D. C. 2010, ApJ, 710, 549
Leonard, P. J. T. 1991, AJ, 101, 562
Miceli, M., Decourchelle, A., Ballet, J., et al. 2008, Adv. Space Res., 41, 390
Mohamed, S., Mackey, J., & Langer, N. 2012, A&A, 541, A1
Noriega-Crespo, A., van Buren, D., & Dgani, R. 1997, AJ, 113, 780
Peri, C. S., Benaglia, P., Brookes, D. P., Stevens, I. R., & Isequilla, N. L. 2012, A&A, 538, A108
Smith, R. K., Brickhouse, N. S., Liedahl, D. A., & Raymond, J. C. 2001, ApJ, 556, L91
Terada, Y., Tashiro, M. S., Bamba, A., et al. 2012, arXiv:1207.5577
van Buren, D., & McCray, R. 1988, ApJ, 329, L93
van Buren, D., Noriega-Crespo, A., & Dgani, R. 1995, AJ, 110, 2914